Journal of Solid State Chemistry **165,** 171–177 (2002)
doi:10.1006/jssc.2001.9528, available online at http://www.idealibrary.com on IDEAL®

Hydrothermal Synthesis and Spectroscopic and Magnetic Behavior of the $Mn_7(HOXO_3)_4(XO_4)_2$(X = As, P) Compounds. Crystal Structure of $Mn_7(HOAsO_3)_4(AsO_4)_2$

José M. Rojo,* Aitor Larrañaga,† José L. Mesa,* Miren K. Urtiaga,† José L. Pizarro,† María I. Arriortua,† and Teófilo Rojo*,[1]

*Departamento de Química Inorgánica and †Departamento de Mineralogía-Petrología, Facultad de Ciencias, Universidad del País Vasco, Apdo. 644, E-48080 Bilbao, Spain

Received October 18, 2001; in revised form January 23, 2002; accepted February 1, 2002

The $Mn_7(HOXO_3)_4(XO_4)_2$ (X = As, P) compounds have been synthesized by using hydrothermal conditions. The arsenate phase was obtained under autogeneous pressure at 170°C. However, more drastic conditions at both pressure and temperature were necessary in the attainment of the phosphate compound. The crystal structure of $Mn_7(HOAsO_3)_4(AsO_4)_2$ was solved using single-crystal data. The unit-cell parameters are $a = 6.810(3)$ Å, $b = 8.239(2)$ Å, $c = 10.011(4)$ Å, $\alpha = 104.31(2)°$, $\beta = 108.94(3)°$, $\gamma = 101.25(2)°$. Triclinic, $P\bar{1}$ with $Z = 1$. The isostructural $Mn_7(HOPO_3)_4(PO_4)_2$ phase was characterized from X-ray powder diffraction techniques. The crystal structure of both compounds consists of zig-zag chains constructed by dimeric edge-sharing Mn_2O_{10} octahedra linked through the MnO_5 trigonal bipyramids. The three-dimensional framework is completed by the connection between isolated MnO_6 entities to the dimers octahedra and trigonal bipyramids. The existence of hydrogenarsenate and hydrogenphosphate anions has been confirmed by IR and Raman spectroscopies. Magnetic measurements indicate the existence of antiferromagnetic interactions in both compounds, which are slightly stronger in the arsenate phase. © 2002 Elsevier Science (USA)

Key Words: **hydrothermal synthesis; crystal structure; magnetic behavior.**

INTRODUCTION

A great challenge in materials sciences is the design of compounds with potential practical applications in fields such as the ion exchange, surface absorption chemistry, ionic conductivity, catalysis, etc. In this way, the transition metal phosphates or arsenates with a three-dimensional condensed framework can give rise to original physical properties, due to the great number of different cation arrangements that they exhibit (1).

In the last few years, it has been tried to design synthetic pathways to obtain phosphated materials with condensed crystal structures (2, 3). At this point, the hydrothermal techniques can be an adequate synthetic method to prepare phosphates or arsenates with complex structural architectures (4, 5). During the course of our studies on the exploratory synthesis of some first-row transition-metal phosphates by hydrothermal methods, we have previously reported the synthesis of $Co_7(HOPO_3)_4(PO_4)_2$ (6). This phase is a member of the $M_7(HOPO_3)_4(PO_4)_2$ (M = Mn, Fe, Co) series of compounds reported in the literature (7–9). Although suitable single crystals for the X-ray structure determination of these phases have been prepared, polycrystalline pure phases were not obtained. This fact precluded carrying out any study on the physical properties of these materials. However, a systematic study of the hydrothermal synthetic conditions allowed us to obtain the best conditions of pressure and temperature to prepare $Co_7(HOPO_3)_4(PO_4)_2$ as a pure phase (6). The magnetic study of this phase revealed an unusual and interesting metamagnetic behavior.

In an attempt to extend the range of phases which adopt this type of structure, hydrothermal reactions analogous to that used to prepare $Co_7(HOPO_3)_4(PO_4)_2$ were carried out using the manganese(II) cation and the phosphate and arsenate oxoanions. This paper describes the results of these reactions, and the structural and spectroscopic and magnetic behaviors of the $Mn_7(HOXO_3)_4(XO_4)_2$ X = As and P compounds. As far as we are aware, the $Mn_7(HOAsO_3)_4(AsO_4)_2$ compound is the first member synthesized from this family with the arsenate group.

EXPERIMENTAL

Synthesis and Characterization

$Mn_7(HOAsO_3)_4(AsO_4)_2$ was prepared by mild hydrothermal conditions under autogeneous pressure starting

[1] To whom correspondence should be addressed. Fax: 34-944648500. E-mail: qiproapt@lg.ehu.es.

0022-4596/02 $35.00

from $MnCl_2 \cdot 4H_2O$ and $NaHAsO_4 \cdot 7H_2O$ in a volume of 30 mL of water. The pH of the reaction mixture was decreased until 4.5 by using HCl, by stirring until homogeneity was reached. After that, the mixture was sealed in a PTFE-lined stainless-steel pressure vessel (fill factor 75%) and heated at 170°C for 5 days, followed by slow cooling to room temperature. The pH was practically constant during the hydrothermal reaction and remained at 4.5. Well-formed light-pink single crystals appeared which were isolated by filtration, washed with water and acetone and dried over P_2O_5 for 2 h.

Attempts to obtain the phosphate phase by using this method were not successful. Hence, more energized hydrothermal conditions were used, increasing both the temperature and pressure in the reaction. The $Mn_5(HOPO_3)_2(PO_4)_2 \cdot 4H_2O$ phase (10) was used as starting precursor to obtain the more compact $Mn_7(HOPO_3)_4(PO_4)_2$ compound. $Mn_5(HOPO_3)_2(PO_4)_2 \cdot 4H_2O$ was prepared refluxing an aqueous solution with $MnCl_2 \cdot 4H_2O$, H_3PO_4 and NaOH at pH of 4.5. The manganese content of $Mn_5(HOPO_3)_2(PO_4)_2 \cdot 4H_2O$ was determined by inductively coupled plasma atomic emission spectroscopy (ICP-AES) analysis, and the percentage of the water molecule calculated by thermogravimetric analysis. Approximately, 0.1 g of $Mn_5(HOPO_3)_2(PO_4)_2 \cdot 4H_2O$ disaggregated in water was sealed in a small gold capsule, and the capsule was then loaded into an externally heated hydrothermal reactor. A number of experimental runs were carried out at temperatures and pressures in the 200–600°C and 300–600 atm ranges, respectively. After 4 days of reaction, a fine polycrystalline solid with light-pink color corresponding to $Mn_7(HOPO_3)_4(PO_4)_2$ was separated by filtration, washed with water and acetone and dried over P_2O_5 for 2 h.

The manganese, arsenic and phosphorus contents of the $Mn_7(HOXO_3)_4(XO_4)_2$ (X = As, P) compounds were confirmed by ICP-AES analysis. Found: Mn, 31.1; As, 36.0. $Mn_7(HOAsO_3)_4(AsO_4)_2$ requires Mn, 31.5; As, 36.8. Found: Mn, 39.8; P, 19.0. $Mn_7(HOPO_3)_4(PO_4)_2$ requires Mn, 40.1; P, 19.4. The density was measured by picnometry. The obtained values are 4.5(4) and 3.7(3) g cm^{-3} for the arsenate and phosphate compounds, respectively.

Thermogravimetric analysis of both compounds was carried out under oxygen atmosphere in an SDC 2960 simultaneous DSC-TGA TA Instrument. Crucibles containing ca. 20 mg of sample were heated at 5°C min^{-1} in the temperature range 30–800°C. The decomposition curves of both phases reveal continuous weight losses in the 380–480 and 440–500°C ranges, which correspond to the decomposition of manganese (II)-arsenate and -phosphate respectively. The X-ray diffraction pattern of the residue obtained from the thermogravimetric analysis at 800°C of the arsenate phase shows the simultaneous presence of $Mn_2As_2O_7$ [$C2/m$ space group with $a = 6.756(1)$ Å, $b = 8.770(1)$ Å, $c = 4.805(1)$ Å and $\beta = 102.8(1)°$] and Mn_2O_3 [$Ia3$ space group with unit cell parameters of 9.43(1) Å] (11a), as main components. In the thermogravimetric residue at 800°C of the phosphate phase, the presence of $Mn_2P_2O_7$ [$C2/m$ space group with $a = 6.633(1)$ Å, $b = 8.584(1)$ Å, $c = 4.546(1)$ Å and $\beta = 120.7(1)°$] and $Mn_3(PO_4)_2$ [$P2_1/c$ space group with $a = 8.940(1)$ Å, $b = 10.040(1)$ Å, $c = 24.140(1)$ Å and $\beta = 120.8(1)°$] (11b) was observed.

X-ray Diffraction Study

A prismatic single crystal of $Mn_7(HOAsO_3)_4(AsO_4)_2$ with dimensions $0.06 \times 0.04 \times 0.04$ mm^3 was used for the data collection performed on an Enraf-Nonius CAD4 automated diffractometer using graphite-monochromated Mo$K\alpha$ radiation. The total number of measured reflections was 3005, with 2857 reflections being independent (Rint. = 0.04) and 2388 observed applying the criterion $I > 2\sigma(I)$. Corrections for Lorentz and polarization effects were done even for absorption taking into account the crystal shape by using the XRED program (12). The structure was solved by direct methods (SHELXS 97) (13). The heavy elements, arsenic and manganese, were first located. The oxygen atoms and as well as the hydrogen atoms belonging to the hydrogenarsenate anions were found in difference Fourier maps. The structure was refined by the full-matrix least-squares method based on F^2, using the SHELXL 97 computer program (14). The scattering factors were taken from Ref. (15). All the non-hydrogen atoms were assigned anisotropic thermal parameters. The final R factors were $R1 = 0.047$ [w$R2 = 0.120$]. Maximum and minimum peaks in final difference synthesis were 1.566 and -2.039 e$Å^{-3}$. All the drawings were made using ATOMS program (16). Crystallographic data, atomic coordinates and selected bond distances and angles are listed in Tables 1, 2 and 3, respectively.

The X-ray powder pattern of $Mn_7(HOPO_3)_4(PO_4)_2$ was refined by the Rietveld method, FULLPROF program (17). The X-ray powder pattern was collected with a PHILIPS X'PERT diffractometer. Details of the procedure concerning the data collection are given in Table 1. The Rietveld full-profile refinement of $Mn_7(HOPO_3)_4(PO_4)_2$ was performed starting from the atomic coordinates obtained from single-crystal data by Riou *et al.* (7). The observed, calculated and difference X-ray powder diffraction patterns are shown in Fig. 1. The obtained results indicate a P-1 triclinic space group and unit-cell parameters similar to those reported in the literature [$a = 6.608(9)$ Å, $b = 8.078(6)$ Å, $c = 9.79(1)$ Å, $\alpha = 112.2(1)°$, $\beta = 110.2(1)°$, and $\gamma = 101.4(1)°$] (7) (see Table 1).

Physicochemical Characterization Techniques

The IR spectra (KBr pellets) were obtained with a Nicolet FT-IR 740 spectrophotometer in the 400–4000 cm^{-1} range.

TABLE 1
Crystallographic Data and the Details of Crystal Structure Refinement for the $Mn_7(HXO_4)_4(XO_4)_2$ (X = As, P) Compounds

Chemical formula	$H_4As_6Mn_7O_{24}$	$H_4P_6Mn_7O_{24}$
a (Å)	6.810(3)	6.604(1)
b (Å)	8.239(2)	8.066(2)
c (Å)	10.011(4)	9.728(2)
α (°)	104.31(2)	104.10(1)
β (°)	108.94(3)	109.66(1)
γ (°)	101.25(2)	101.27(1)
V (Å^3)	491.0(3)	450.9(2)
Z	1	1
Formula weight (g mol^{-1})	1222.13	958.41
Space group	P-1 (no. 2)	P-1 (no. 2)
T (°C)	20	20
Radiation	λ(Mo$K\alpha$), 0.71070 Å	λ(Cu$K\alpha$), 1.5418 Å
ρ_{obs}, ρ_{calc} (g cm^{-3})	4.5(4), 4.13	3.7(3), 3.50
μ (Mo$K\alpha$) (mm^{-1})	14.509	46.685
R ($I > 2\sigma(I)$]	$R1 = 0.047$ w$R2 = 0.120$	
R [all data]	$R1 = 0.056$ w$R2 = 0.130$	
2θ range (°)		10–90
2θ step-scan increment (°)		0.02
Time-step (s/step)		12
No. of reflections/independents		1606/724
No. of structural parameters		55
No. of profile parameters		14
R_p		14.7
R_{wp}		19.6
R_B		15.2
χ^2		2.68

Note. $R1 = [\sum(|F_o| - |F_c|)]/\sum|F_o|$; w$R2 = [\sum(w(|F_o|^2 - |F_c|^2)^2]/\sum[w(|F_o|^2)^2]^{1/2}$; $w = 1/[\sigma^2|F_o|^2 + (xp)^2]$; where $p = [|F_o|^2 + 2|F_c|^2]/3$; $x = 0.0804$.
$R_p = \sum|yi_{obs} - (1/c)yi_{calc}|/\sum yi_{obs}$; $R_{wp} = [\sum\omega i|yi_{obs} - (1/c)yi_{calc}|^2/\sum\omega i[yi_{obs}]^2]^{1/2}$.
$R_B = \sum|I_{obs} - I_{calc}|/\sum I_{obs}$.

The Raman spectra were recorded in the 200–3000 cm^{-1} range, with a Nicolet 950FT spectrophotometer equipped with a neodymium laser emitting at 1064 nm. A Bruker ESP 300 spectrometer was used to record the ESR polycrystalline spectra. The temperature was stabilized by an Oxford Instrument (ITC 4) regulator. The magnetic field was measured with a Bruker BNM 200 gaussmeter and the frequency inside the cavity was determined using a Hewlett-Packard 5352B microwave frequency counter. Magnetic measurements on powdered sample were performed in the temperature range 2.0–300 K, using a Quantum Design MPMS-7 SQUID magnetometer. The magnetic field was approximately 0.1 T, a value in the range of linear dependence of magnetization vs magnetic field even at 2.0 K.

RESULTS AND DISCUSSION

Crystal Structure of $Mn_7(HOAsO_3)_4(AsO_4)_2$

The crystal structure of $Mn_7(HOAsO_3)_4(AsO_4)_2$ consists of a three-dimensional framework formed by MnO_6 octahedra, MnO_5 trigonal bipyramids and $HOAsO_3$ and AsO_4 tetrahedra (Fig. 2a).

Zig-zig chains running along the [10-1] direction are present in the structural network (Fig. 2b). The chains are constructed from $Mn(2)_2O_{10}$ and $Mn(4)_2O_{10}$ dimeric edge-sharing octahedra linked in alternated way through $Mn(3)O_5$ trigonal bipyramids, which share an edge with the octahedral polyhedra. The chains are connected along the [101] direction by $Mn(1)O_6$ octahedra. Every $Mn(1)O_6$ octahedron is simultaneously bonded to two $Mn(2)O_6$ octahedra, through the O(6)-oxygen atoms, and to two $Mn(3)O_5$ trigonal bipyramids, through the O(10)-oxygen atoms, giving rise to the three-dimensional network of this complex structure (Fig. 2c).

The Mn(2) cations of the condensed $Mn(2)_2O_{10}$ octahedra are bonded to the O(5) and two O(1) atoms from the $As(2)O_4$ arsenate groups and to the O(6), O(9) and O(7) atoms belonging to the $HOAs(1)O_3$ ad $HOAs(3)O_3$ hydrogenarsenate anions, respectively. The mean Mn(2)-O distance is of 2.18(5) Å. The common edge between the $Mn(2)O_6$ octahedra is formed by the O(1)–O(1)^{ii} atoms from the $As(2)O_4$ tetrahedron. In the dimeric $Mn(4)_2O_{10}$ octahedra, the Mn(4) ions share the O(8)-oxygen atoms belonging to the $As(2)O_4$ group, with the coordination sphere completed by the O(3), O(12) and O(4), O(11) atoms from the $HOAs(1)O_3$ and $HOAs(3)O_3$ hydrogenarsenate anions, respectively. The mean value of the Mn(4)–O distances is 2.16(3) Å. The Mn(1) cation in the $Mn(1)O_6$ octahedron is

TABLE 2
Atomic Coordinates ($\times 10^4$) and Equivalent Temperature Factors (Å$^2\times 10^3$) for $Mn_7(HAsO_4)_4(AsO_4)_2$ (e.s.d. in Parentheses)

Atom	x	y	z	U_{eq}
Mn(1)	0	5000	0	8(1)
Mn(2)	3844(1)	9557(1)	1126(1)	7(1)
Mn(3)	7154(1)	6845(1)	7143(1)	8(1)
Mn(4)	9422(1)	7837(1)	4836(1)	8(1)
As(1)	2283(1)	6473(1)	7814(1)	5(1)
As(2)	859(1)	754(1)	8256(1)	5(1)
As(3)	4095(1)	7321(1)	3732(1)	6(1)
O(1)	3108(6)	10265(5)	−870(4)	8(1)
O(2)	1126(7)	2904(5)	−972(5)	11(1)
O(3)	10080(7)	6752(6)	6614(5)	10(1)
O(4)	6216(7)	6946(6)	4911(5)	12(1)
O(5)	1325(6)	10475(5)	1627(5)	8(1)
O(6)	2215(7)	6884(5)	−467(4)	9(1)
O(7)	4847(7)	8977(6)	3157(5)	13(1)
O(8)	10488(7)	10400(5)	6447(4)	8(1)
O(9)	5391(6)	12512(5)	2263(5)	9(1)
O(10)	2504(7)	5474(5)	2325(4)	9(1)
O(11)	12669(7)	7981(6)	4808(5)	12(1)
O(12)	7949(7)	5738(5)	2733(5)	11(1)

Note. $U_{eq} = (1/3)[U_{11}(aa^*)^2 + U_{22}(bb^*)^2 + U_{33}(cc^*)^2 + 2U_{12}aba^*b^*\cos\gamma + 2U_{13}aca^*c^*\cos\beta + 2U_{23}bcb^*c^*\cos\alpha]$.

TABLE 3
Selected Bond Distances (Å) and Angles (°) for $Mn_7(HAsO_4)_4(AsO_4)_2$ (e.s.d. in Parentheses)

Bond distances (Å)			
Mn(1)O_6 *octahedron*		*Mn*(2)O_6 *octahedron*	
Mn(1)–O(2)	2.165(4)	Mn(2)–O(7)	2.129(4)
Mn(1)–O(2)^{i}	2.165(4)	Mn(2)–O(1)	2.151(4)
Mn(1)–O(6)	2.193(4)	Mn(2)–O(1)^{ii}	2.155(4)
Mn(1)–O(6)^{i}	2.193(4)	Mn(2)–O(5)	2.155(4)
Mn(1)–O(10)^{i}	2.279(4)	Mn(2)–O(6)	2.187(4)
Mn(1)–O(10)	2.279(4)	Mn(2)–O(9)	2.277(4)
Mn(3)O_6 *trigonal bipyramid*		*Mn*(4)O_6 *octahedron*	
Mn(3)–O(5)^{iii}	2.098(4)	Mn(4)–O(8)	2.132(4)
Mn(3)–O(9)^{iii}	2.124(4)	Mn(4)–O(12)	2.140(4)
Mn(3)–O(10)^{iv}	2.141(4)	Mn(4)–O(3)	2.143(4)
Mn(3)–O(4)	2.143(4)	Mn(4)–O(8)^{v}	2.168(4)
Mn(3)–O(3)	2.232(4)	Mn(4)–O(4)	2.195(4)
		Mn(4)–O(11)	2.201(4)
HOAs(1)O_3 *tetrahedron*		*As*(2)O_4 *tetrahedron*	
As(1)–O(9)^{iii}	1.676(4)	As(2)–O(1)^{viii}	1.679(4)
As(1)–O(3)^{vi}	1.688(4)	As(2)–O(5)^{ix}	1.684(4)
As(1)–O(6)^{vii}	1.688(4)	As(2)–O(8)^{x}	1.686(4)
As(1)–O(12)^{iv}	1.727(4)	As(2)–O(2)^{vii}	1.696(4)
HOAs(3)O_3 *tetrahedron*		*metal–metal*	
As(3)–O(7)	1.662(4)	Mn(1)–Mn(2)^{i}	3.7917(7)×2
As(3)–O(10)	1.667(4)	Mn(1)–Mn(3)^{iv,xi}	3.7347(9)
As(3)–O(4)	1.680(4)	Mn(2)–Mn(2)^{ii}	3.281(1)
As(3)–O(11)^{vi}	1.730(4)	Mn(2)–Mn(3)^{iii}	3.356(1)
		Mn(3)–Mn(4)	3.338(1)
		Mn(4)–Mn(4)^{v}	3.404(1)
Bond angles (°)			
Mn(1)O_6 *octahedron*		*Mn*(2)O_6 *octahedron*	
O(2)–Mn(1)–O(2)^{i}	180.0	O(7)–Mn(2)–O(1)	175.2(2)
O(2)–Mn(1)–O(6)	90.3(2)	O(7)–Mn(2)–O(1)^{ii}	95.2(2)
O(2)^{i}–Mn(1)–O(6)	89.7(2)	O(1)–Mn(2)–O(1)^{ii}	80.7(2)
O(2)–Mn(1)–O(6)^{i}	89.7(2)	O(7)–Mn(2)–O(5)	90.9(2)
O(2)^{i}–Mn(1)–O(6)^{i}	90.3(2)	O(1)–Mn(2)–O(5)	92.0(1)
O(6)–Mn(1)–O(6)^{i}	180.0	O(1)^{ii}–Mn(2)–O(5)	157.4(2)
O(2)–Mn(1)–O(10)^{i}	89.2(2)	O(7)–Mn(2)–O(6)	99.3(2)
O(2)^{i}–Mn(1)–O(10)^{i}	90.8(2)	O(1)–Mn(2)–O(6)	83.5(2)
O(6)–Mn(1)–O(10)^{i}	86.9(1)	O(1)^{ii}–Mn(2)–O(6)	94.8(2)
O(6)^{i}–Mn(1)–O(10)^{i}	93.1(1)	O(5)–Mn(2)–O(6)	105.7(2)
O(2)–Mn(1)–O(10)	90.8(2)	O(7)–Mn(2)–O(9)	94.6(2)
O(2)^{i}–Mn(1)–O(10)	89.2(2)	O(1)–Mn(2)–O(9)	82.4(2)
O(6)–Mn(1)–O(10)	93.1(1)	O(1)^{ii}–Mn(2)–O(9)	82.1(1)
O(6)^{i}–Mn(1)–O(10)	86.9(1)	O(5)–Mn(2)–O(9)	75.7(1)
O(10)^{i}–Mn(1)–O(10)	180.0	O(6)–Mn(2)–O(9)	165.9(1)
Mn(3)O_5 *trigonal bipyramid*		*Mn*(4)O_6 *octahedron*	
O(5)^{iii}–Mn(3)–O(9)^{iii}	80.2(2)	O(8)–Mn(4)–O(12)	160.7(2)
O(5)^{iii}–Mn(3)–O(10)^{iv}	132.2(2)	O(8)–Mn(4)–O(3)	89.7(2)
O(9)^{iii}–Mn(3)–O(10)^{iv}	106.7(2)	O(12)–Mn(4)–O(3)	109.0(2)
O(5)^{iii}–Mn(3)–O(4)	99.9(2)	O(8)–Mn(4)–O(8)^{v}	75.3(2)
O(9)^{iii}–Mn(3)–O(4)	101.9(2)	O(12)–Mn(4)–O(8)^{v}	86.7(2)
O(10)^{iv}–Mn(3)–O(4)	123.4(2)	O(3)–Mn(4)–O(8)^{v}	163.0(2)
O(5)^{iii}–Mn(3)–O(3)	88.9(2)	O(8)–Mn(4)–O(4)	97.7(2)
O(9)^{iii}–Mn(3)–O(3)	168.4(2)	O(12)–Mn(4)–O(4)	82.6(2)
O(10)^{iv}–Mn(3)–O(3)	83.6(2)	O(3)–Mn(4)–O(4)	76.7(2)
O(4)–Mn(3)–O(3)	75.9(2)	O(8)^{v}–Mn(4)–O(4)	112.7(2)
		O(8)–Mn(4)–O(11)	93.7(2)
		O(12)–Mn(4)–O(11)	90.5(2)
		O(3)–Mn(4)–O(11)	91.5(2)
		O(8)^{v}–Mn(4)–O(11)	81.7(2)
		O(4)–Mn(4)–O(11)	163.4(2)
HOAs(1)O_3 *tetrahedron*		*As*(2)O_3 *tetrahedron*	
O(9)^{iii}–As(1)–O(3)^{vi}	112.6(2)	O(1)^{viii}–As(2)–O(5)^{ix}	110.4(2)
O(9)^{iii}–As(1)–O(6)^{vii}	116.3(2)	O(1)^{viii}–As(2)–O(8)^{x}	109.2(2)
O(3)^{vi}–As(1)–O(6)^{vii}	110.5(2)	O(5)^{ix}–As(2)–O(8)^{x}	110.3(2)
O(9)^{iii}–As(1)–O(12)^{iv}	105.8(2)	O(1)^{viii}–As(2)–O(2)^{vii}	110.9(2)
O(3)^{vi}–As(1)–O(12)^{iv}	107.7(2)	O(5)^{ix}–As(2)–O(2)^{vii}	108.7(2)
O(6)^{vii}–As(1)–O(12)^{iv}	103.0(2)	O(8)^{x}–As(2)–O(2)^{vii}	107.2(2)
HOAs(3)O_3 *tetrahedron*			
O(7)–As(3)–O(10)	113.1(2)		
O(7)–As(3)–O(4)	112.8(2)		
O(10)–As(3)–O(4)	110.5(2)		
O(7)–As(3)–O(11)^{vi}	106.5(2)		
O(10)–As(3)–O(11)^{vi}	109.0(2)		
O(4)–As(3)–O(11)^{vi}	104.4(2)		

Note. Symmetry codes i = $-x, -y+1, -z$, ii = $-x+1, -y+2, -z$, iii = $-x+1, -y+2, -z+1$, iv = $-x+1, -y+1, -z+1$, v = $-x+2, -y+2, -z+1$, vi = $x-1, y, z$, vii = $x, y, z+1$, viii = $x, y-1, z+1$, ix = $-x, -y+1, -z+1$, $x = x-1, y-1, z$, xi = $x-1, y, z-1$.

bonded to the O(2) atoms from the arsenate and to the O(6) and O(10) atoms belonging to the hydrogenarsenates, with a mean bond distance of 2.21(5) Å. In these coordination polyhedra, the *cis*- and *trans*-O–Mn–O angles are those usually found for an octahedral geometry. The distortion of these polyhedra from the ideal octahedral symmetry, calculated on the basis of Muetterties and Guggenberger model (18), is smaller than 8%. In the $Mn(3)O_5$ trigonal bipyramid, the Mn(3) ions are bonded to the O(4), O(10)^{iv}

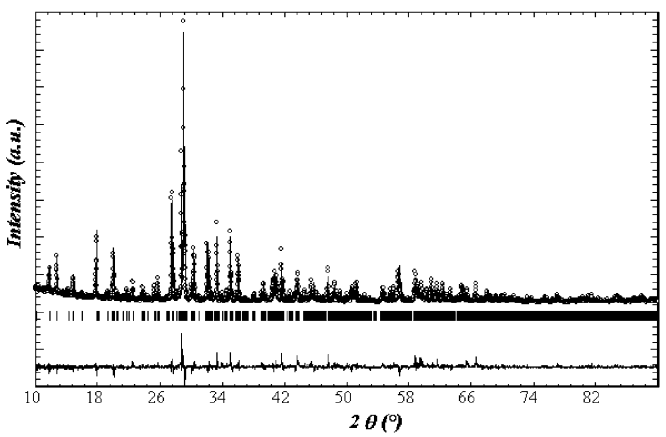

FIG. 1. The observed, calculated and difference X-ray powder diffraction patterns of $Mn_7(HOPO_3)_4(PO_4)_2$. The observed data are shown by the circles, the calculated diffractogram by the solid line, and the difference spectrum in the lower region.

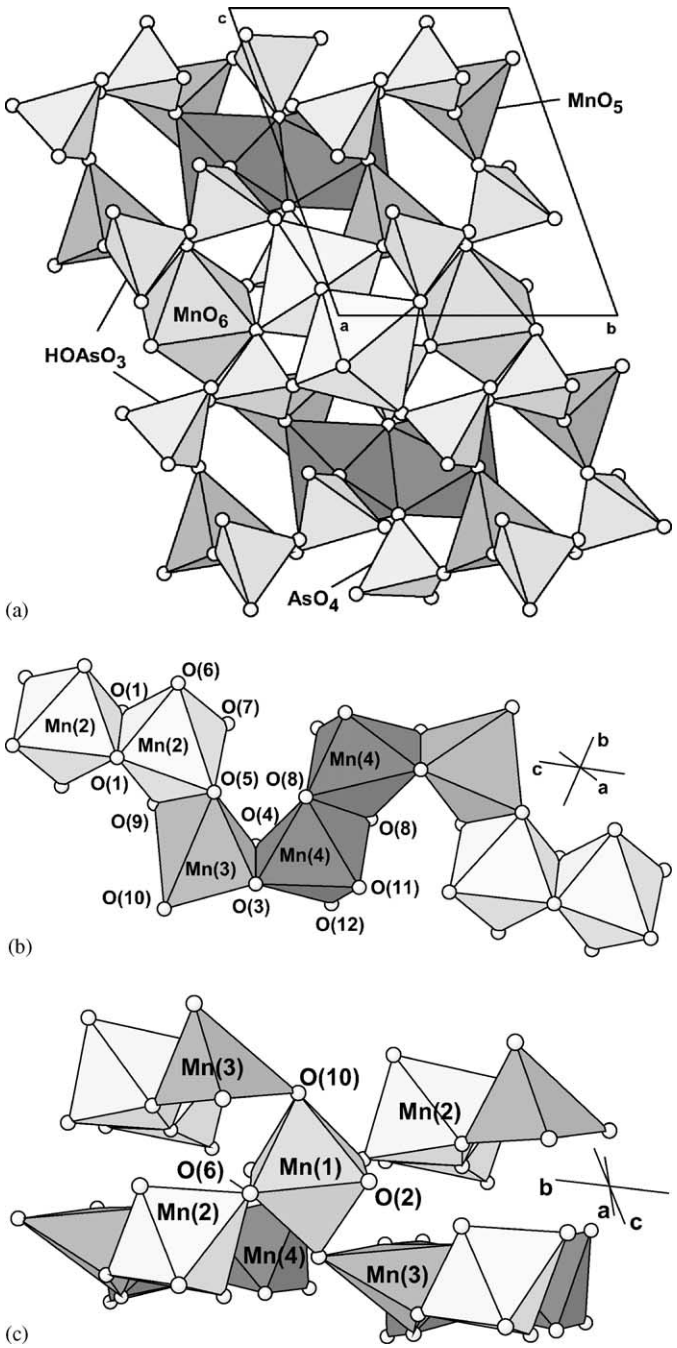

FIG. 2. (a) Polyhedral view of the crystal structure of $Mn_7(HOAsO_3)_4(AsO_4)_2$. (b) Chains of $Mn_7(HOAsO_3)_4(AsO_4)_2$ along the [1 0 -1] direction, showing the Mn_2O_{10} edge-sharing dimeric octahedra and the MnO_5 trigonal bipyramids. (c) Chains of $Mn_7(HOAsO_3)_4(AsO_4)_2$ linked through the $Mn(1)O_6$ octahedra.

atoms, from the $HOAs(3)O_3$ group, and to the $O(5)^{iii}$-oxygen, from the $As(2)O_4$ tetrahedron, forming the equatorial plane. The O(3) and $O(9)^{iii}$ atoms, belonging to the $HOAs(1)O_3$ anion, occupy the axial positions of the trigonal bipyramid. In this polyhedron, the mean manganese–oxygen distance is 2.15(4) Å, and its distortion from the square pyramidal geometry is ca. 20% (18).

The O(11)–As(3) and O(12)–As(1) bond distances in the hydrogenarsenate anions exhibit a mean value of 1.728(5) Å, which is slightly greater than that observed in the arsenate groups [1.68(1) Å]. Thus, the O(11)- and O(12)-oxygen atoms complete their electrostatic valence through the link to the H(11)- and H(12)-hydrogen atoms from the hydrogenarsenate anions. The O–As–O angles are those usually found for an sp^3 hybridation.

The unit-cell parameters for the $M_7(HOXO_3)_4(XO_4)_2$ (M = Mn, Fe, Co; X = P, As) compounds are presented in Table 4. The unit-cell volume shows a linear increase from the iron to the manganese compound, according to the increase of the ionic radii of the elements (Fig. 3). The evolution of the molecular-weight/volume ratio is consistent with the variation observed in the density of the compounds. The high value of the density obtained for the arsenate phase can be related to the difference in the atomic weight between the phosphorus and arsenic elements, which is not compensated by the difference in the ionic radii.

Infrared and Raman Spectroscopies

The Infrared and Raman spectra of the $Mn_7(HOXO_3)_4(XO_4)_2$ (X = As and P) phases show the same features. The spectra exhibit the bands corresponding to the vibrations of the $(HOXO_3)^{2-}$ and $(XO_4)^{3-}$ anions. The stretching ν(HOAs) and bending δ(HOAs) modes appear at frequencies of 2425 and 1305 cm^{-1} in the IR spectrum. The asymmetric stretching vibration, ν_{as}(AsO) is observed as a splitted band at 870, 830 cm^{-1}, whereas the symmetric stretching mode, ν_s(AsO) is observed at 755 cm^{-1}. In the Raman spectrum, these modes are

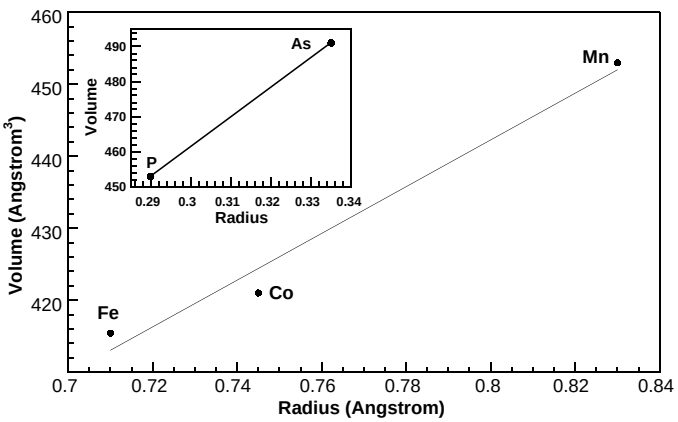

FIG. 3. Variation of the unit-cell volume vs ionic radii for the $M_7(HOXO_3)_4(XO_4)_2$ (M = Fe, Co; X = P and M = Mn; X = P, As) compounds. The ionic radius considered for the iron phosphate compound is the mean value of that of the Fe(II) and Fe(III) cations, according to the composition of this phase (9).

observed at 865, 845 and 735 cm^{-1}, respectively. The deformation δ_{as}(OAsO) mode is centered at approximately 450 cm^{-1} in both IR and Raman spectra. The bands observed in the IR spectrum of the phosphate phase at frequencies of 2865 and 1320 cm^{-1} correspond to the stretching and bending modes of the HO–P groups in the hydrogenphosphate anions, respectively. The asymmetric stretching vibration of the P–O bonds in the IR and Raman spectra appears as a broad splitted band in the 1075–900 and 1060–900 cm^{-1} ranges, respectively. The symmetric stretching mode is detected as a shoulder at ca. 810 cm^{-1} in IR spectroscopy but it was not clearly observed in the Raman spectrum. Finally, the IR and Raman spectra show the δ_{as}(OPO) deformation mode centered at approximately 550 cm^{-1}. These results are similar to those found in the literature for other arsenate and phosphate compounds (19).

ESR and Magnetic Behavior

The ESR spectra of the $Mn_7(HOXO_3)_4(XO_4)_2$ (X = As, P) compounds were performed at X-band on powdered sample at room temperature and 4.2 K. The spectra exhibit quasi-isotropic signals as a result of the collapse between the MnO_6 and MnO_5 chromophores present in the structure. The g-value for both compounds is 2.00(1), which remains unchanged with the variation in temperature. This result is in good agreement with the presence of high-spin Mn(II) cations.

Magnetic measurements of the $Mn_7(HOXO_3)_4(XO_4)_2$ (X = As and P) compounds were performed on powdered sample from room temperature to 2.0 K. The thermal evolution of the χ_m and $\chi_m T$ curves is presented in Fig. 4. The molar magnetic susceptibility, χ_m, of both compounds increases with decreasing temperature and reaches a maximum at 9.5 and 6.0 K, for the arsenate and phosphate compounds, respectively, after which the susceptibility decreases continuously with cooling the sample. Above ca. 20 K, the thermal variation of the molar susceptibility follows a Curie–Weiss law [$\chi_m = C_m/(T - \theta)$] with values of the Curie and Curie–Weiss constants of 30.7, 30.8 cm^3 $K\,mol^{-1}$ and -33.0, -31.8 K, for the arsenate and phosphate phases, respectively. The $\chi_m T$ vs T curves decrease continuously from room temperature which indicates, together with the negative Weiss-temperature, the existence of antiferromagnetic interactions in these compounds. However, both the temperature at which the maximum appears in the χ_m vs T curve of the arsenate phase, and the more negative Weiss constant indicate that the antiferromagnetic interactions are slightly stronger in the arsenate than in the phosphate compound.

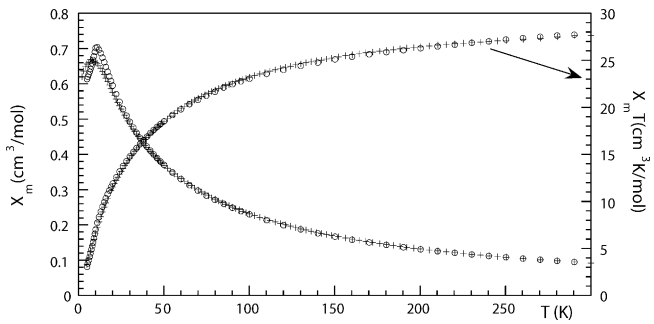

FIG. 4. Thermal variation of the χ_m and $\chi_m T$ curves for the $Mn_7(HOXO_3)_4(XO_4)_2$ [X = As (circles), P (crosses)] compounds.

Considering the structural features in the $Mn_7(HOXO_3)_4(XO_4)_2$ (X = As and P) compounds (see Figs. 2a and 2b), several magnetic exchange pathways can take place: (i) Intradimeric and octahedral–trigonal bipyramid direct interactions involving d_{xz} orbitals Mn^{2+} from the Mn(2), Mn(4) and Mn(3) along the chains. (ii) Superexchange intradimer interactions via oxygen involving metal $d_{x^2-y^2}$ orbitals from edge-sharing $Mn(2)O_6$ and $Mn(4)O_6$ octahedra and between these polyhedra and the $Mn(3)O_5$ trigonal bipyramids along the chains. (iii) Superexchange interactions via vertex oxygen atoms between Mn(1), Mn(2), Mn(3) and Mn(4) ions in the three-dimensional framework. (iv) Superexchange interactions through the HXO_4 and XO_4 groups which are linked to the MnO_6 and MnO_5 polyhedra in three dimensions.

The values of the bond angles involved in these exchange pathways for the $Mn_7(HOXO_3)_4(XO_4)_2$ (X = As, P) compounds and also for $Co_7(HOPO_3)_4(PO_4)_2$ (6) are shown in Table 4. These bond angles with values greater than 90° for exchange pathways (ii) and (iii) should lead to antiferromagnetic interactions that are predominant in these compounds (20). Furthermore, the manganese-arsenate compound exhibits bond angles slightly greater than those found in the manganese-phosphate phase. This result agrees with that obtained from the magnetic measurements, which shows a slightly stronger antiferromagnetic behavior for the $Mn_7(HOAsO_3)_4(AsO_4)_2$ compound. The bond angles of the cobalt-phosphate have values intermediate between those found for both manganese compounds. This fact and the anisotropy characteristic of the Co(II) ion could be responsible for the metamagnetic behavior observed in the $Co_7(HOAsO_3)_4(AsO_4)_2$ compound (6).

Finally, the superexchange pathways through the oxoanions should favor the antiferromagnetic couplings, as observed in other related compounds (21). The direct intermetallic interactions should also lead to antiferromagnetic couplings, because the dihedral angles between the planes which contain the metallic cations have a mean value of ca. 170° for both the arsenate and phosphate compounds. This fact was also observed for the cobalt phase. Thus, it is possible to conclude that these results are in accordance with the antiferromagnetic behavior obtained from the

TABLE 4

Crystallographic parameters and selected angles (°) related to the possible magnetic exchange pathways for the $M_7(HOXO_3)_4(XO_4)_2$ (M = Mn, Fe, Co; X = P, As)

Parameters	Fe-phosphate[a]	Co-phosphate[a]	Mn-phosphate	Mn-arsenate
a (Å)	6.389(2)	6.462(1)	6.604(1)	6.810(3)
b (Å)	7.971(1)	7.864(1)	8.066(2)	8.239(2)
c (Å)	9.531(1)	9.473(2)	9.728(2)	10.011(4)
α (°)	111.16(2)	104.31(2)	104.11(1)	104.31(2)
β (°)	113.07(1)	109.11(2)	109.66(1)	108.94(3)
γ (°)	101.60(2)	101.34(1)	101.27(1)	101.25(2)
V (Å^3)	415(1)	421(1)	451(1)	491(1)
Z	1	1	1	1
ρ	3.69	3.88	3.50	4.13
M. weight/vol.	2.3131	2.3428	2.1157	2.4890

Angle	Mn-arsenate	Mn-phosphate	Co-phosphate
M(2)–O(1)–M(2)^{ii}	99.3(2)	94.8(2)	94.97(7)
M(4)–O(8)–M(4)^{v}	104.7(2)	101.7(2)	102.13(9)
M(3)^{iii}–O(9)–M(2)	99.3(2)	96.3(1)	96.60(6)
M(3)^{iii}–O(5)–M(2)	104.2(2)	101.5(2)	101.40(6)
M(4)–O(3)–M(3)	99.4(2)	96.1(1)	97.14(7)
M(3)–O(4)–M(4)	100.6(2)	97.9(2)	99.45(6)
M(2)–O(6)–M(1)	119.9(2)	115.1(1)	117.51(9)
M(3)^{iv}–O(10)–M(1)	115.3(2)	109.8(1)	112.71(6)

[a] From Refs. (7–9).

magnetic measurements for the $Mn_7(HOXO_3)_4(XO_4)_2$ (X = As, P) compounds.

CONCLUDING REMARKS

The hydrothermal synthesis under autogeneous pressure has allowed to obtain the $Mn_7(HOAsO_3)_4(AsO_4)_2$ new compound in the form of single crystals. The isostructural phosphate phase has been prepared by using more energized temperature and pressure conditions. The structure of these compounds consists of a complex three-dimensional network formed by isolated Mn_2O_{10} octahedra dimers and MnO_5 trigonal bipyramids. IR and Raman spectroscopies have been used to confirm the presence of the hydrogenarsenate or -phosphate anions in the compounds. Magnetic measurements indicate the existence of antiferromagnetic couplings as the main magnetic interactions. The angles involved in the possible exchange pathways are in good agreement with the antiferromagnetic behavior of these phases.

ACKNOWLEDGMENTS

This work was financially supported by the Ministerio de Educación y Ciencia and Universidad del País Vasco/EHU (grants PB97-0640 and 169.310-EB149/98, respectively), which we gratefully acknowledge. One of us A. Larrañaga wishes to thank the Gobierno Vasco/Eusko Jaurlaritza for funding.

REFERENCES

1. (a) S. M. Kauzlarich, P. K. Dorhout, and J. M. Honig, *J. Solid State Chem.* **149,** 3 (2000); (b) D. E. C. Corbridge, "The Structural Chemistry of Phosphorus." Elsevier, Amsterdam, 1974.
2. (a) H. V. Der Meer, *Acta Crystallogr. B* **32,** 2423 (1976); (b) M. Bagieu-Beucher and J. C. Guitel, *Acta Crystallogr. B* **33,** 2529 (1977); (c) I. M. Watson, M. M. Borel, J. Chardon, and A. Leclaire, *J. Solid State Chem.* **111,** 253 (1994); (d) W. T. A. Harrison, *Acta Crystallogr. C* **50,** 1643 (1994); (e) M. Gruss and R. Glaum, *Acta Crystallogr. C* **52,** 2647 (1996); (f) J. M. Rojo, J. L. Mesa, L. Lezama, and T. Rojo, *J. Mater. Chem.* **7**(11), 2243 (1997).
3. (a) J. M. Winand, A. Rulmont, and P. Tarte, *J. Solid State Chem.* **87,** 83 (1990); (b) W. M. Reiff, J. H. Zhang, H. Tam, J. P. Attfield, and C. C. Torardi, *J. Solid State Chem.* **130,** 147 (1997); (c) C. Masquelier, C. Wurm, J. Rodriguez-Carvajal, J. Gaubicher, and L. Nazar, *Chem. Mater.* **12,** 525 (2000); (d) J. L. Mesa, A. Goñi, A. L. Brandl, N. O. Moreno, G. E. Barberis, and T. Rojo, *J. Mater. Chem.* **10,** 2779 (2000).
4. (a) J. L. Pizarro, M. I. Arriortua, L. Lezama, T. Rojo, and G. Villeneuve, *Solid State Ionics* **63–65,** 71 (1993); (b) M. D. Marcos, P. Amoros, D. Beltran, A. Beltran, and J. P. Attfield, *J. Mater. Chem.* **5,** 917 (1995).
5. (a) "Proceedings of the XXXIX European High Pressure Research Group Meeting, Santander, Spain, 2001;" (b) J. M. Rojo, J. L. Mesa, J. L. Pizarro, J. Garcia-Tojal, L. Lezama, M. I. Arriortua, and T. Rojo, *High Pressure Research*, (2002), in press.
6. J. M. Rojo, J. L. Mesa, L. Lezama, J. Rodriguez-Fernandez, J. L. Pizarro, M. I. Arriortua, and T. Rojo, *Int. J. Inorg. Mater.* **3,** 67 (2001).
7. A. Riou, Y. Cudennec, and Y. Gerault, *Acta Crystallogr. C* **43,** 821 (1987).
8. P. Lightfoot and A. K. Cheetham, *Acta Crystallogr. C* **44,** 1331 (1988).
9. Y. Vencato, L. F. Moreiras, E. Mattievich, and Y. Primerano, *J. Braz. Chem. Soc.* **5,** 43 (1994).
10. H. S. Amorin, M. R. Amaral, L. F. Moreiras, and E. Mattievich, *J. Mater. Sci. Lett.* **15,** 1895 (1996).
11. (a) Powder Diffraction File—Inorganic and Organic, "ICDD, Files No. 80-2349 and 78-390." Pennsylvania, USA, 1995; (b) Powder Diffraction File—Inorganic and Organic, "ICDD, Files No. 77–1244, 73-1088." Pennsylvania, USA, 1995.
12. XRED. "Stoe & Cie GmbH." Darmstadt, Germany, 1998.
13. G. M. Sheldrick, "SHELXS 97: Program for the Solution of Crystal Structures." University of Göttingen, Germany, 1997.
14. G. M. Sheldrick, "SHELXL 97: Program for the Refinement of Crystal Structures." University of Göttingen, Germany, 1997.
15. "International Tables for X-ray Crystallography," Vol. IV, p. 99. Kynoch Press, Birmingham, England, 1974.
16. E. Dowty, "ATOMS: A Computer Program for Displaying Atomic Structures." Shape Software, 521 Hidden Valley Road, Kingsport, TN, 1993.
17. J. Rodriguez-Carvajal, "FULLPROF, Program for Rietveld Pattern Matching Analysis of Powder Patterns." ILL Grenoble, 1994, unpublished.
18. E. L. Muetterties and L. J. Guggenberger, *J. Am. Chem. Soc.* **96,** 1748 (1974).
19. K. Nakamoto, "Infrared and Raman Spectra of Inorganic and Coordination Compounds." John Wiley & Sons, New York, 1997.
20. J. B. Goodenough, "Magnetism and the Chemical Bond." Interscience, New York, 1963.
21. L. Lezama, K. S. Shu, G. Villeneuve, and T. Rojo, *Solid State Commun.* **76,** 449 (1990).